Eur. Phys. J. B (2015) 88: 182
DOI: 10.1140/epjb/e2015-60361-5

THE EUROPEAN PHYSICAL JOURNAL B

Regular Article

Temperature dependence of thermal conductivities of coupled rotator lattice and the momentum diffusion in standard map

Yunyun Li[1], Nianbei Li[1,a], and Baowen Li[1,2,3,b]

[1] Center for Phononics and Thermal Energy Science, School of Physical Sciences and Engineering, Tongji University, Shanghai 200092, P.R. China
[2] Department of Physics and Centre for Computational Science and Engineering, National University of Singapore, Singapore 117546, Republic of Singapore
[3] Center for Advanced 2D Material and Graphene Research Centre, National University of Singapore, Singapore 117542, Republic of Singapore

Received 5 May 2015 / Received in final form 21 May 2015
Published online 13 July 2015 –

Abstract. In contrary to other 1D momentum-conserving lattices such as the Fermi-Pasta-Ulam β (FPU-β) lattice, the 1D coupled rotator lattice is a notable exception which conserves total momentum while exhibits normal heat conduction behavior. The temperature behavior of the thermal conductivities of 1D coupled rotator lattice had been studied in previous works trying to reveal the underlying physical mechanism for normal heat conduction. However, two different temperature behaviors of thermal conductivities have been claimed for the same coupled rotator lattice. These different temperature behaviors also intrigue the debate whether there is a phase transition of thermal conductivities as the function of temperature. In this work, we will revisit the temperature dependent thermal conductivities for the 1D coupled rotator lattice. We find that the temperature dependence follows a power law behavior which is different with the previously found temperature behaviors. Our results also support the claim that there is no phase transition for 1D coupled rotator lattice. We also give some discussion about the similarity of diffusion behaviors between the 1D coupled rotator lattice and the single kicked rotator also called the Chirikov standard map. It is found that the momentum diffusion constant for 1D coupled rotator lattice follows a power-law temperature dependence of $T^{-3.2}$ which is close to that of Chirikov standard map which follows a behavior of T^{-3}.

1 Introduction

The exploration of underlying mechanism for anomalous and normal heat conduction in low dimensional systems represents a huge challenge in the area of statistical physics [1–4]. After enormous efforts for more than one decade from numerical simulation [5–44], theoretical predictions [45–57] and experimental observations [58–60], there is still no consensus for the exact physical mechanism causing anomalous heat conduction. It is believed that momentum conservation plays an important role in determining the actual heat conduction behavior. In general, 1D non-integrable lattices with momentum conserving property should have anomalous heat conduction where the thermal conductivity κ diverges with the lattice size N as $\kappa \propto N^{\alpha}$ where $0 < \alpha < 1$ [1–4]. However, the 1D coupled rotator lattice is a well-known exception. It exhibits normal heat conduction behavior despite its momentum conserving nature [61,62].

The normal heat conduction in 1D coupled rotator lattice was discovered via numerical simulations by two groups independently [61,62]. In order to understand the underlying mechanism, the temperature dependence of thermal conductivity has been studied in detail in both works. In reference [61], the temperature dependence of thermal conductivity of coupled rotator lattice has been found to be like $\kappa(T) \propto e^{\Delta V/T}$ where ΔV is a positive constant proportional to the barrier height of the potential energy. However, in reference [62], a temperature dependence of thermal conductivity of $\kappa(T) \propto e^{-T/A}$ was claimed where A is a positive constant. There it was also argued that a possible phase transition at temperature around $T \sim 0.2$–0.3 where heat conduction is normal above this temperature while anomalous below this temperature exists [62]. Although this phase transition statement was challenged as a finite size effect [63,64], a later work supported this phase transition conjecture after deriving a similar temperature dependent thermal conductivity as $\kappa(T) \propto e^{-T/A}$ [50].

Most recently, the 1D coupled rotator lattice reattracts much attention due to the new finding of simultaneously existing normal diffusion of momentum as well as normal diffusion of heat energy [65]. It is argued that the normal behavior might be due to the reduced number of

[a] e-mail: nbli@tongji.edu.cn
[b] e-mail: phononics@tongji.edu.cn

conserved quantities which is unique for periodic interaction potentials [66,67]. But the new debate is that whether the stretch is conserved or not in 1D coupled rotator lattice. The investigation of 1D coupled rotator lattice will be the key to unravel the true mechanism behind the connection between momentum conservation and normal or anomalous heat conduction. Therefore, it is timely to revisit the temperature dependence of thermal conductivity of 1D coupled rotator lattice as a first step.

In this work, we will revisit the temperature dependence of thermal conductivities for the 1D coupled rotator lattice. We find that the temperature dependence is neither $\kappa(T) \propto e^{\Delta V/T}$ nor $\kappa(T) \propto e^{-T/A}$ as previously claimed [61,62]. The actual temperature dependence is a power-law dependence as $\kappa(T) \propto T^{-3.2}$. The possible connection with the momentum diffusion of single kicked rotator or the Chirikov standard map has also been discussed. In order to determine whether there is a phase transition, we also present the temperature dependent thermal conductance at different system sizes. All the thermal conductances for different sizes collapse to the same value at low temperatures while approach to the power-law behavior as $\kappa(T) \propto T^{-3.2}$ at high temperatures. However, the crossover temperature decreases as the system size increases. This fact indicates that there is no phase transition between normal and anomalous heat conduction. In thermodynamical limit, the heat conduction is normal for all temperatures except the trivial zero temperature point. In Section 2 the lattice model and numerical methods will be introduced. Numerical results and discussions will be presented in Section 3 and the results will be summarized in Section 4.

2 Model and numerical methods

The Hamiltonian for the 1D coupled rotator lattice is defined as the following [61,62]:

$$H = \sum_{i=1}^{N} \left[\frac{p_i^2}{2} + K[1 - \cos(q_{i+1} - q_i)] \right] \tag{1}$$

where q_i and p_i denote the displacement from equilibrium and momentum for ith atom, respectively. The mass of the atom m and the Boltzmann constant k_B has been set into unity. The parameter K with energy dimension represents the coupling strength of the inter-atom potential. Therefore, the system temperature T can be rescaled by T/K and we can also set $K = 1$ for simplicity [68]. The equations of motion for ith atom are

$$\begin{aligned} \dot{q}_i &= p_i \\ \dot{p}_i &= K \sin(q_{i+1} - q_i) - K \sin(q_i - q_{i-1}). \end{aligned} \tag{2}$$

At low temperature limit, the displacements are small values so that $|q_{i+1} - q_i| \ll 1$. The Hamiltonian can be expanded into the Taylor series as:

$$H = \sum_{i=1}^{N} \left[\frac{p_i^2}{2} + \frac{(q_{i+1} - q_i)^2}{2} - \frac{(q_{i+1} - q_i)^4}{4!} + \frac{(q_{i+1} - q_i)^6}{6!} - \dots \right]. \tag{3}$$

This Hamiltonian will approach to the integrable Harmonic lattice only at zero temperature $T = 0$. The first stable nonlinear potential term will be the sextic potential.

On the other hand, at infinite high temperature limit $T = \infty$, the rotator lattice will approach to another integrable system consisting of N independent and isolated free particles as

$$H = \sum_{i=1}^{N} \frac{p_i^2}{2}. \tag{4}$$

This is because the kinetic energy is proportional to the temperature as $\langle p_i^2 \rangle = T$ and the potential energy in equation (1) is confined by the cosine function.

Without getting into numerics, we can get a qualitative picture of the thermal conductivity of 1D coupled rotator lattice as the function of temperature. The thermal conductivity $\kappa(T)$ will diverge in the low temperature limit approaching to the harmonic limit and will decay to zero in the high temperature limit as approaching to the unconnected N free particles. As a general picture, the thermal conductivity $\kappa(T)$ will decrease as the temperature increases.

For numerical simulations, we will use both non-equilibrium molecular dynamics (NEMD) and equilibrium molecular dynamics (EMD) methods. In the NEMD method, the first and last atoms are put into contact with the left and right Langevin heat baths with temperature $T_{L/R}$ and fixed boundary conditions with $q_0 = q_{N+1} = 0$ are applied. The equations of motion for the lattice are:

$$\begin{aligned} \ddot{q}_i &= -\sin(q_i) + \sin(q_{i+1} - q_i) - \lambda \dot{q}_i + \xi_i, \ i = 1 \\ \ddot{q}_i &= -\sin(q_i - q_{i-1}) + \sin(q_{i+1} - q_i), \ i = 2, \dots, N-1 \\ \ddot{q}_i &= -\sin(q_i - q_{i-1}) + \sin(-q_i) - \lambda \dot{q}_i + \xi_i, \ i = N \end{aligned} \tag{5}$$

and the Gaussian white noise $\xi_1(t)$ and $\xi_N(t)$ satisfy

$$\langle \xi_{1/N}(t) \rangle = 0, \ \langle \xi_{1/N}(t) \xi_{1/N}(0) \rangle = 2\lambda k_B T_{L/R} \delta(t) \tag{6}$$

where T_L and T_R are the temperature for the left and right Langevin heat baths and λ is the coupling strength. The temperatures are set as $T_{L/R} = T(1 \pm \Delta)$ where T denotes the average temperature and Δ gives rise to the temperature gradient along the lattice, and is chosen as $\Delta = 0.1$ in our simulations. In the dimensionless units, the coupling strength λ is set to be $\lambda = 1$ which is not too large and not too small. The equations of motion of equation (5) will be integrated with the second order Verlet velocity algorithm and the time step Δt is chosen as $\Delta t = 0.01$ in dimensionless unit. The temperature profile and thermal conductivity in the next section will be calculated using the NEMD method.

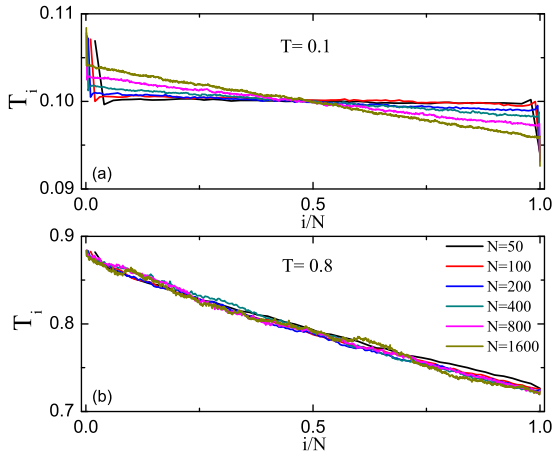

Fig. 1. Temperature profiles for the 1D coupled rotator lattice at (a) $T = 0.1$ and (b) $T = 0.8$. The lattice sizes are $N = 50, 100, 200, 400, 800$ and 1600 and the color rules of the lines are the same for both (a) and (b). The first and last atoms are put into contact with Langevin heat baths with temperature set as $T_{L/R} = T(1 \pm \Delta)$ where $\Delta = 0.1$ here.

In the EMD method, there is no heat bath and the periodic boundary conditions $q_i = q_{i+N}$ are applied. The equations of motion for the lattice can be simply expressed as

$$\ddot{q}_i = -\sin(q_i - q_{i-1}) + \sin(q_{i+1} - q_i), \ i = 1, \ldots, N. \quad (7)$$

The average energy density is the input parameter and the temperature need to be calculated as $T = T_i = \langle p_i^2 \rangle$ where $\langle \cdot \rangle$ denotes time average which is equivalent to the ensemble average due to the chaotic nature of the coupled rotator lattice. The equations of motion of equation (7) will be integrated with fourth order symplectic algorithm [69,70] which is more accurate and the time step $\Delta t = 0.1$ will be used. The momentum diffusion constant in the next section will be calculated via the EMD method.

3 Results and discussions

Before we discuss the results of thermal conductivities, we first show the temperature profiles. In Figure 1, the temperature profiles at two different temperatures $T = 0.1$ and $T = 0.8$ are plotted. The lattice sizes are chosen as $N = 50, 100, 200, 400, 800$ and 1600. For relative low temperature at $T = 0.1$, the temperature jumps at two boundaries are obvious. However, the temperature jumps are reduced with the increase of lattice size N as can be seen in Figure 1a. In Figure 1b where the temperature is relatively high at $T = 0.8$, all the temperature profiles collapse to the same straight line as the temperature jumps are very small for all lattice sizes.

In order to obtain the temperature dependence of thermal conductivities, we need first define the way how $\kappa(T)$ can be calculated numerically. We notice that the temperature profiles all collapse to the same straight line if the temperature jumps can be ignored at high temperatures

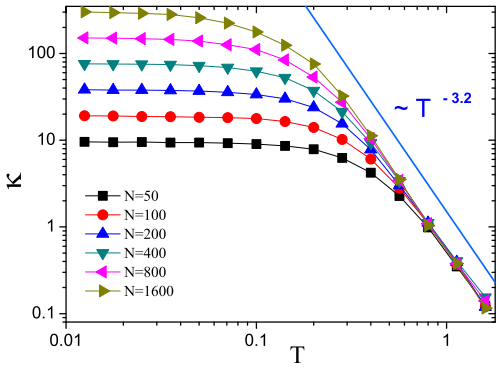

Fig. 2. Thermal conductivities $\kappa(T)$ as the function of temperature for different lattice sizes $N = 50, 100, 200, 400, 800$ and 1600. The straight line is proportional to $T^{-3.2}$ which describes the temperature behavior of $\kappa(T)$ at high temperature region very well.

or long lattice sizes. It is appropriate to define the thermal conductivity $\kappa(T)$ as:

$$\kappa(T) = \frac{JN}{T_L - T_R} \quad (8)$$

where $J = \langle J_i \rangle$ is the average heat flux along the lattice in the stationary state and the local heat flux J_i is defined as $J_i = -p_i K \sin(q_{i+1} - q_i)$ via the energy continuity equation.

In Figure 2, the thermal conductivities $\kappa(T)$ as the function of temperature are plotted for different lattice sizes $N = 50, 100, 200, 400, 800$ and 1600. At high temperature region, all the thermal conductivities $\kappa(T)$ for different lattice sizes collapse together indicating the saturation of thermal conductivities as the increase of lattice size. This is characteristic for lattices with normal heat conduction. As the temperature decreases, the thermal conductivities first increases and then becomes flat. This is because the phonon mean free paths are getting longer as the temperature reduces and the ballistic regime will be approached if the phonon mean free paths are longer than the lattice size. The boundary jumps will dominate the temperature profiles as in Figure 1a and the definition of $\kappa(T)$ of equation (8) will no longer reflect the actual thermal conductivities.

At high temperatures, it is clearly seen that the thermal conductivities follow a power-law dependence as $\kappa(T) \propto T^{-3.2}$. For the longest size we considered here as $N = 1600$, this power-law behavior can be best fitted for more than two orders of magnitudes for the $\kappa(T)$ value as shown in Figure 3. This also explains the poor fitting of the $\kappa(T) \propto e^{\Delta V/T}$ dependence in reference [61] and the $\kappa(T) \propto e^{-T/A}$ dependence in reference [62].

This power-law dependence of $\kappa(T) \propto T^{-3.2}$ cannot be explained by the effective phonon theory which is able to predict the temperature dependent thermal conductivities for other typical 1D nonlinear lattices such as FPU-β lattice and generalized nonlinear Klein-Gordon lattices [71–78]. According to the effective phonon theory, the thermal conductivity for low temperature rotator

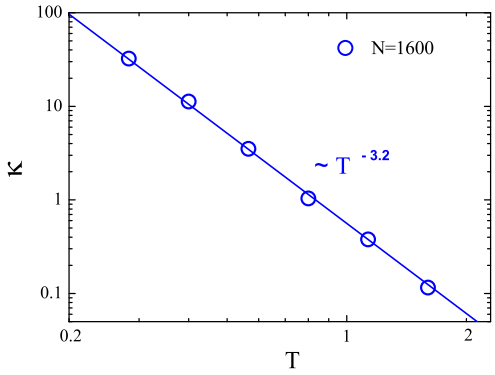

Fig. 3. Thermal conductivities $\kappa(T)$ as the function of temperature for lattice size $N = 1600$. The data are taken from Figure 2 and can be best fitted to be a power-law dependence as $\kappa(T) \propto T^{-3.2}$.

lattice with Hamiltonian of equation (3) can be derived as

$$\kappa(T) \propto \frac{1}{\epsilon} \propto T^{-2} \tag{9}$$

where ϵ is the nonlinearity strength with the following temperature dependence

$$\epsilon \propto \frac{\langle (q_{i+1} - q_i)^6 \rangle}{\langle (q_{i+1} - q_i)^2 \rangle} \propto T^2 \tag{10}$$

at low temperature region. Here we consider the sextic potential term as the lowest nonlinear term because the dynamics governed by the negative quartic potential term is unstable. Therefore, the actual temperature behavior of $\kappa(T) \propto T^{-3.2}$ is steeper than the prediction of $\kappa(T) \propto T^{-2}$ from effective phonon theory.

Although it is difficult to unravel the exact physical mechanism behind the power-law dependence of thermal conductivities for coupled rotator lattice, it is very helpful to look into the transport properties of the single kicked rotator (the Chirikov standard map) [79]. As the name indicates, the coupled rotator lattice is a kind of connected kicked rotators. The equations of motion for the single kicked rotator are

$$\begin{aligned} p_{n+1} - p_n &= K \sin(q_n) \\ q_{n+1} - q_n &= p_{n+1} \end{aligned} \tag{11}$$

where q_n and p_n denote the coordinate and momentum after nth kick.

The variation of momentum p is unbounded and can be characterized by a normal diffusion [79,80]

$$\langle \Delta p^2(t) \rangle \sim 2Dt \tag{12}$$

where D is the diffusion constant. This is similar to the normal momentum diffusion for 1D coupled rotator lattice. According to references [79,80], the diffusion constant D depends on the coupling strength K as:

$$D \propto (K - 1.2)^3, \quad 1.2 < K < 4 \tag{13}$$

$$D \propto K^2, \quad K > 4 \tag{14}$$

where 1.2 is the chaos threshold for the kicked rotator.

If one assumes the transport properties of coupled rotator lattice are the same as that of single kicked rotator, one would expect that the energy diffusion constant D_E as well as the momentum diffusion constant D_P of coupled rotator lattice should also follow the same dependence as that of single kicked rotator as in equation (13). To translate the K dependence into T dependence, we notice that the parameter K in single kicked rotator of equation (11) plays the same role as that in the coupled rotator lattice as in equation (2). As we have discussed above, the dynamics of coupled rotator lattice can be rescaled with T/K. The K dependence should be inversely proportional to the T dependence. Low K value region corresponds to the high T region and vice verse. For normal heat conduction, the thermal conductivity κ is proportional to the energy diffusion constant D_E. This will finally give rise to the prediction of temperature dependent thermal conductivity $\kappa(T)$ of coupled rotator lattice from the analogy with single kicked rotator:

$$\kappa(T) \propto T^{-2}, \quad \text{low } T \tag{15}$$

$$\kappa(T) \propto T^{-3}, \quad \text{high } T. \tag{16}$$

As a consistence check, we calculate the momentum diffusion constant D_P for the coupled rotator lattice with EMD method. According to reference [27], one can define the momentum fluctuation correlation function $C_P(r,t)$ as

$$C_P(r = i - j, t) = \frac{\langle p_i(t) p_j(0) \rangle}{\langle p_j(0) p_j(0) \rangle} \tag{17}$$

where j is the reference atom and $r = i - j$ denotes the distance from the reference atom. The momentum diffusion process can be measured by the mean square displacement as

$$\langle r^2(t) \rangle_P = \sum_r r^2 C_P(r,t). \tag{18}$$

The momentum diffusion of 1D coupled rotator lattice is normal [65], therefore, a momentum diffusion constant D_P can be defined as

$$D_P = \lim_{t \to \infty} \frac{\langle r^2(t) \rangle_P}{2t}. \tag{19}$$

In Figure 4, we plot the momentum diffusion constant D_P for the coupled rotator lattice as the function of temperature. The same temperature dependence of $D_P \propto T^{-3.2}$ has been obtained.

Therefore, the prediction of $\kappa(T) \propto T^{-3}$ with analogy to the single kicked rotator at high temperature or low K region is close to the numerical observation of $\kappa(T) \propto T^{-3.2}$. This indicates there might be some deeper connection between the diffusion behavior of single kicked rotator and 1D coupled rotator lattice. In addition, the analogy analysis also predicts a $\kappa(T) \propto T^{-2}$ behavior at low temperature region which is the same as the prediction from the effective phonon theory of equation (9). The reason why this temperature behavior cannot be observed in numerical simulations might be due to the severe finite size effect at low temperature region as can be seen in Figure 1a.

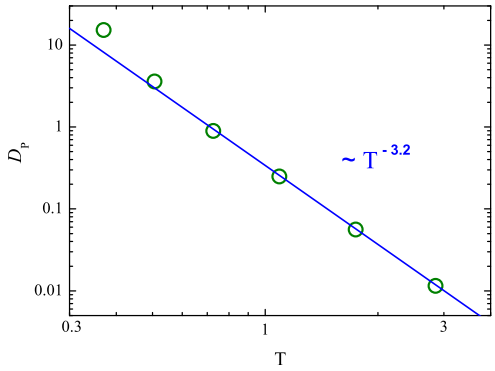

Fig. 4. Momentum diffusion constant D_P as the function of temperature for 1D coupled rotator lattice. The numerical data are obtained via equilibrium MD simulations as in reference [65]. The solid line of $T^{-3.2}$ is guided for the eye.

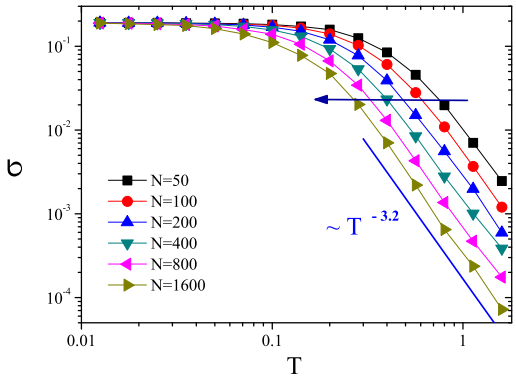

Fig. 5. Heat conductance σ as the function of temperature T for different lattice size $N = 50, 100, 200, 400, 800$ and 1600. All the other parameters are the same as in Fig. 2. The left-pointing arrow represents the trend of decreasing crossover temperature as the lattice size increases.

In the final part we will discuss the issue about the possible phase transition between normal and anomalous heat conduction for 1D coupled rotator lattice. As we have shown in Figure 3, the actual temperature dependence of $\kappa(T)$ is a power-law dependence as $\kappa(T) \propto T^{-3.2}$. This indicates the analytic derivation of $\kappa(T) \propto e^{-T/A}$ in reference [50] originally for a lattice with pinned on-site potential can not be extended to 1D coupled rotator lattice.

On the other hand, the claim that the transition temperature is around (0.2–0.3) in reference [62] has been challenged in references [63,64] with numerical simulations of larger sizes. The possible phase transition could be a finite size effect. Here we reconfirm the finite size effect by giving a more illustrative picture in Figure 5. The heat conductance $\sigma(T, N) \equiv \kappa(T)/N$ for different sizes N collapse to a common value given by the harmonic limit in the low temperature limit while approaching the power-law temperature behavior of $\sigma \propto T^{-3.2}$ at high temperature regime. As the temperature decreases, the phonon mean free path will overcome the lattice size and the heat conductance will saturate to a value determined by the harmonic limit of coupled rotator lattice. As can be seen from Figure 5, the heat conductance for short lattice will first bend and become flat as the temperature decreases. This crossover temperature decreases as the lattice size increases smoothly and no sign of phase transition can be observed. It is also noticed that the crossover temperature happens to be around (0.2–0.3) for lattice sizes of a few thousands. Therefore, our results also indicate that there is no phase transition between normal and anomalous heat conduction for the 1D coupled rotator lattice. In thermodynamical limit as $N \to \infty$, the heat conduction should be normal for all temperatures except the trivial zero temperature point.

4 Summary

We have systematically investigated the temperature dependence of thermal conductivities of 1D coupled rotator lattice. The actual temperature dependence is a power-law dependence of $\kappa(T) \propto T^{-3.2}$ which is different with the observations of previous studies. The possible connection with the single kicked rotator or the Chirikov standard map has been discussed where a $\kappa(T) \propto T^{-3}$ dependence can be implied. Our results also reconfirm that the previously claimed possible phase transition should be a finite size effect.

The numerical calculations were carried out at Shanghai Supercomputer Center. This work has been supported by the NSF China with Grant No. 11334007 (Y.L., N.L., B.L.), the NSF China with Grant No. 11347216 (Y.L), Tongji University under Grant No. 2013KJ025 (Y.L), the NSF China with Grant No. 11205114 (N.L.), the Program for New Century Excellent Talents of the Ministry of Education of China with Grant No. NCET-12-0409 (N.L.) and the Shanghai Rising-Star Program with Grant No. 13QA1403600 (N.L.).

References

1. S. Lepri, R. Livi, A. Politi, Phys. Rev. Lett. **78**, 1896 (1997)
2. S. Lepri, R. Livi, A. Politi, Phys. Rep. **377**, 1 (2003)
3. A. Dhar, Adv. Phys. **57**, 457 (2008)
4. S. Liu, X. Xu, R. Xie, G. Zhang, B. Li, Eur. Phys. J. B **85**, 337 (2013)
5. B. Hu, B. Li, H. Zhao, Phys. Rev. E **57**, 2992 (1998)
6. P. Tong, B. Li, B. Hu, Phys. Rev. B **59**, 8639 (1999)
7. T. Hatano, Phys. Rev. E **59**, R1 (1999)
8. G.P. Tsironis, A.R. Bishop, A.V. Savin, A.V. Zolotaryuk, Phys. Rev. E **60**, 6610 (1999)
9. A. Sarmiento, R. Reigada, A.H. Romero, K. Lindenberg, Phys. Rev. E **60**, 5317 (1999)
10. A. Dhar, D. Dhar, Phys. Rev. Lett. **82**, 480 (1999)
11. D. Alonso, R. Artuso, G. Casati, I. Guarneri, Phys. Rev. Lett. **82**, 1859 (1999)
12. B. Hu, B. Li, H. Zhao, Phys. Rev. E **61**, 3828 (2000)
13. K. Aoki, D. Kusnezov, Phys. Lett. A **265**, 250 (2000)
14. B. Li, H. Zhao, B. Hu, Phys. Rev. Lett. **86**, 63 (2001)
15. A. Dhar, Phys. Rev. Lett. **86**, 5882 (2001)
16. K. Aoki, D. Kusnezov, Phys. Rev. Lett. **86**, 4029 (2001)

17. Y. Zhang, H. Zhao, Phys. Rev. E **66**, 026106 (2002)
18. B. Li, L. Wang, B. Hu, Phys. Rev. Lett. **88**, 223901 (2002)
19. K. Saito, Europhys. Lett. **61**, 34 (2003)
20. A.V. Savin, O.V. Gendelman, Phys. Rev. E **67**, 041205 (2003)
21. S. Lepri, R. Livi, A. Politi, Phys. Rev. E **68**, 067102 (2003)
22. D. Segal, A. Nitzan, P. Hänggi, J. Chem. Phys. **119**, 6840 (2003)
23. O.V. Gendelman, A.V. Savin, Phys. Rev. Lett. **92**, 074301 (2004)
24. B. Li, J. Wang, L. Wang, G. Zhang, Chaos **15**, 015121 (2005)
25. G. Zhang, B. Li, J. Chem. Phys. **123**, 114714 (2005)
26. H. Zhao, Z. Wen, Y. Zhang, D. Zheng, Phys. Rev. Lett. **94**, 025507 (2005)
27. H. Zhao, Phys. Rev. Lett. **96**, 140602 (2006)
28. D. He, S. Buyukdagli, B. Hu, Phys. Rev. E **78**, 061103 (2008)
29. Z.-G. Shao, L. Yang, W.-R. Zhong, D.-H. He, B. Hu, Phys. Rev. E **78**, 061130 (2008)
30. Y. Dubi, M. Di Ventra, Phys. Rev. E **79**, 042101 (2009)
31. A. Henry, G. Chen, Phys. Rev. B **79**, 144305 (2009)
32. K. Saito, A. Dhar, Phys. Rev. Lett. **104**, 040601 (2010)
33. L. Wang, D. He, B. Hu, Phys. Rev. Lett. **105**, 160601 (2010)
34. N. Yang, G. Zhang, B. Li, Nano Today **5**, 85 (2010)
35. L. Wang, T. Wang, Europhys. Lett. **93**, 54002 (2011)
36. L. Wang, B. Hu, B. Li, Phys. Rev. E **86**, 040101 (2012)
37. D. Xiong, J. Wang, Y. Zhang, H. Zhao, Phys. Rev. E **85**, 020102(R) (2012)
38. G.T. Landi, M.J. de Oliveira, Phys. Rev. E **87**, 052126 (2013)
39. D. Xiong, Y. Zhang, H. Zhao, Phys. Rev. E **90**, 022117 (2014)
40. S.G. Das, A. Dhar, K. Saito, C.B. Mendl, H. Spohn, Phys. Rev. E **90**, 012124 (2014)
41. C.B. Mendl, H. Spohn, Phys. Rev. E **90**, 012147 (2014)
42. A.V. Savin, Y.A. Kosevich, Phys. Rev. E **89**, 032102 (2014)
43. S. Liu, J. Liu, P. Hänggi, C. Wu, B. Li, Phys. Rev. B **90**, 174304 (2014)
44. L. Wang, L. Xu, H. Zhao, Phys. Rev. E **91**, 012110 (2015)
45. S. Lepri, R. Livi, A. Politi, Europhys. Lett. **43**, 271 (1998)
46. S. Lepri, Phys. Rev. E **58**, 7165 (1998)
47. O. Narayan, S. Ramaswamy, Phys. Rev. Lett. **89**, 200601 (2002)
48. J.-S. Wang, B. Li, Phys. Rev. Lett. **92**, 074302 (2004)
49. P. Cipriani, S. Denisov, A. Politi, Phys. Rev. Lett. **94**, 244301 (2005)
50. E. Pereira, R. Falcao, Phys. Rev. Lett. **96**, 100601 (2006)
51. L. Delfini, S. Lepri, R. Livi, A. Politi, Phys. Rev. E **73**, 060201 (2006)
52. G. Basile, C. Bernardin, S. Olla, Phys. Rev. Lett. **96**, 204303 (2006)
53. H. van Beijeren, Phys. Rev. Lett. **108**, 180601 (2012)
54. C.B. Mendl, H. Spohn, Phys. Rev. Lett. **111**, 230601 (2013)
55. E. Pereira, R. Falcao, H.C.F. Lemos, Phys. Rev. E **87**, 032158, (2013)
56. H. Spohn, J. Stat. Phys. **154**, 1191 (2014)
57. S. Liu, P. Hänggi, N. Li, J. Ren, B. Li, Phys. Rev. Lett. **112**, 040601 (2014)
58. C.W. Chang, D. Okawa, H. Garcia, A. Majumdar, A. Zettl, Phys. Rev. Lett. **101**, 075903 (2008)
59. X. Xu, L.F.C. Pereira, Y. Wang, J. Wu, K. Zhang, X. Zhao, S. Bae, C.T. Bui, R. Xie, J.T.L. Thong, B.H. Hong, K.P. Loh, D. Donadio, B. Li, B. Ozyilmaz, Nat. Commun. **5**, 3689 (2014)
60. T. Meier, F. Menges, P. Nirmalraj, H. Hölscher, H. Riel, B. Gotsmann, Phys. Rev. Lett. **113**, 060801 (2014)
61. C. Giardina, R. Livi, A. Politi, M. Vassalli, Phys. Rev. Lett. **84**, 2144 (2000)
62. O.V. Gendelman, A.V. Savin, Phys. Rev. Lett. **84**, 2381 (2000)
63. L. Yang, B. Hu, Phys. Rev. Lett. **94**, 219404 (2005)
64. L. Yang, P. Grassberger, `arXiv:cond-mat/0306173` (2003)
65. Y. Li, S. Liu, N. Li, P. Hänggi, B. Li, New J. Phys. **17**, 043064 (2015)
66. S.G. Das, A. Dhar, `arXiv:1411.5247v2` (2015)
67. H. Spohn, `arXiv:1411.3907` (2014)
68. N. Li, J. Ren, L. Wang, G. Zhang, P. Hänggi, B. Li, Rev. Mod. Phys. **84**, 1045 (2012)
69. J. Laskar, P. Robutel, Celest. Mech. Dyn. Astron. **80**, 39 (2001)
70. Ch. Skokos, D.O. Krimer, S. Komineas, S. Flach, Phys. Rev. E **79**, 056211 (2009)
71. N. Li, P. Tong, B. Li, Europhys. Lett. **75**, 49 (2006)
72. N. Li, B. Li, Europhys. Lett. **78**, 34001 (2007)
73. N. Li, B. Li, Phys. Rev. E **76**, 011108 (2007)
74. N. Li, B. Li, J. Phys. Soc. Jpn **78**, 044001 (2009)
75. N. Li, B. Li, S. Flach, Phys. Rev. Lett. **105**, 054102 (2010)
76. N. Li, B. Li, AIP Adv. **2**, 041408 (2012)
77. N. Li, B. Li, Phys. Rev. E **87**, 042125 (2013)
78. L. Yang, N. Li, B. Li, Phys. Rev. E **90**, 062122 (2014)
79. B.V. Chirikov, Phys. Rep. **52**, 263 (1979)
80. R.S. MacKay, J.D. Meiss, I.C. Percival, Physica D **13**, 55 (1984)